

Cascade Model Predictive Current Control for Five-Phase Permanent Magnet Synchronous Motor

SHU XIONG¹ AND JIANGCHENG LI²

¹School of Physics and Electronics Electrical Engineering, Huaiyin Normal University, Jiangsu 223300, China

²State Grid Huai'an Power Supply Company, Jiangsu 223300, China


Corresponding author: Shu Xiong (xiongshuok@163.com)

ABSTRACT As to the model predictive control for five-phase permanent magnet synchronous motor (PMSM), it is difficult to ensure the optimal control performance by using calculation method to obtain the weighting factor. To solve this problem, a cascade model predictive current control based on the idea of sequential model predictive control is proposed for five-phase PMSM for the first time. Firstly, the principle of selecting the optimal voltage vector by the proposed method is analyzed in detail. Then, combined with the characteristics of five-phase PMSM, the control priority of controlled variables is set for designing two cost function schemes without weighting factor. The maximum torque scheme can generate a trapezoidal stator voltage, improving the DC bus voltage utilization rate and the system loading capacity. The minimum harmonic current scheme can reduce the harmonic of stator current, obtaining small system noise and vibration. The experimental results indicate that the proposed method can ensure the optimality of the voltage vector applied. Therefore, the five-phase PMSM obtains good performance under different working operation, such as small torque ripple, fast dynamic response, and small harmonic current.

INDEX TERMS Five-phase permanent magnet synchronous motor, model predictive current control, weighting factor, voltage vector.

I. INTRODUCTION

Permanent magnet synchronous motor (PMSM) is broadly used in industrial production, such as wind power, electric locomotive, and numerical control machine tool [1]. Under the background of vigorous expansion in new energy application technology, the electric drive system composed of multi-phase PMSM and buck-boost power converter caters to the development trend of new energy [2], [3]. Due to the increase of the phase number of stator winding, multi-phase PMSM can normally work despite two of the bridge arm broken. Thus, multi-phase PMSM has a strong ability in reliability and fault tolerance and the characteristics of large output power with low voltage and low torque ripple. Multi-phase PMSM can meet the needs of high performance AC transmission in power, safety, and reliability, enjoying a broad application prospect in new energy electric vehicle and electric propulsion aircraft [4], [5].

The associate editor coordinating the review of this manuscript and approving it for publication was Alexander Micallef .

As an advanced control method, model predictive control (MPC) becomes a hot research topic in recent years. A large number of study results indicate that MPC is an emerging high performance control method for AC motor that can be seen as an alternative version of vector control and direct torque control [6], [7]. According to optimization problem solution, MPC is divided into finite control set model predictive control (FCS-MPC) and continuous set model predictive control [8]. Based on the discrete mathematical model of the inverter, FCS-MPC can select an optimal one from a limited number of switching states through enumeration method. Therefore, the modulator used to generate PWM (pulse width modulation) driving signal is removed in FCS-MPC. Meanwhile, the nonlinear problem of the inverter can be well solved [9].

Due to simple implementation and fast dynamic response, FCS-MPC is very suitable for controlling multivariable and nonlinear PMSM [10]. Model predictive torque control (MPTC) and model predictive current control (MPCC) are two basic FCS-MPC methods for PMSM. In the two

control approaches, the key technologies for implementation are the use of prediction model to calculate the future state of the system and the cost function to select an optimal voltage vector balancing the performance of flux and torque in MPCC and that of d-axis current and q-axis stator current in MPCC.

For a PMSM to tend to be stable, it is necessary to properly design the weighting factor in the cost function because of the distinct dimension of the controlled variables. Nevertheless, the current research indicates that it is still difficult to establish the mathematical relation between the weighting factor and the controlled variable. For this reason, the weighting factor is mainly obtained by the trial and error method that repeats adjustment in simulation or experiment rather than analytical method [11], [12]. The trial and error method is with the advantages of complex operation and poor universality. For example, the weighting factor should be changed with system parameter and operating state. Therefore, the adjustment of weighting factor is a research problem in FCS-MPC, thereby limiting the application and development of FCS-MPC in the field of motor control [13], [14].

To solve the problem mentioned above, calculation method and elimination method are developed presently [15]. The essence of calculation method is a mathematical optimization method applying to multi-variables system difficult to eliminate the weighting factor. R. Vargas proposed a dynamic adjustment method [16] to ensure the weighting factor changes with the error of the controlled variable. The results show that the penalty force for the controlled variable has a dynamical change, and thus the system error can be controlled within a certain range. P. Cortes adopted several interpolation operations to fast determine the weighting factor, obtaining an excellent control performance [17]. It is not difficult to find that the two methods above only improve the efficiency of matching weighting factor, but still do not get rid of the cumbersome process in trial and error. In [18] and [19], the combination of artificial intelligence with motor control makes the use of artificial neural network (ANN) to weighting factor calculation possible. The simulation model or experimental result is used to train ANN. The trained ANN is able to calculate the performance index of the weighting factor and find the optimal weighting factor with the expected performance of the system. However, ANN training is very time-consuming and requires manual intervention.

To avoid the weighting factor participating in the decision-making of system performance optimization, the elimination method is to indirectly transform the cost function or unify controlled variable. R. S. Dastjerdi improves PMSM control performance through the idea of model replacement [20]. The stator flux and torque are replaced with dq-axis stator voltage that has the same dimension, eliminating the weighting factor of stator flux. However, some approximate equivalence in model replacement reduces the control accuracy. In [21], the candidate voltage vectors are ranked according to the errors of flux and torque, without using weighting factor to the select optimal voltage vector. However, ignoring relative errors of flux and torque amplitude, the method proposed

in [21] is difficult to ensure PMSM has the optimal control performance. In 2019, IEEE life fellow also the MPC expert Rodriguez proposed a sequential MPC [22]. The stator flux and torque are included in two independent cost functions, respectively. Two optimal voltage vectors are first selected by the torque cost function, and then evaluated by the flux cost function to obtain an optimal one. It is concluded that the voltage vector is separately selected by the cost functions of stator flux and torque without using weighting factor. Since it was proposed, sequential MPC has attracted the attention of scholars and been successively applied to three-phase PMSM and asynchronous motor and power converter [23], [24].

Based on the principle of the sequential MPC, a cascade MPCC is proposed for five-phase PMSM for the first time to solve the problems of cumbersome weighting factor adjustment. Firstly, taking the stator fundamental dq-axis currents and third harmonic dq-axis currents of the five-phase PMSM as the controlled variables, the proposed method selects the optimal voltage vector for the four controlled variables by constructing two independent cost functions. Secondly, the construction scheme of cost function can change with the system performance requirement. The maximum torque scheme can improve the DC voltage utilization and output electromagnetic torque while the harmonic elimination scheme can reduce the third harmonic in stator current. Therefore, the proposed method can not only solve the problem of weighting factor design, but also realize the maximum torque and minimum harmonic controls for five-phase PMSM. In addition, the sector judgment and one-step delay compensation methods are used to reduce the amount of calculation and improve the control accuracy. Finally, the control performance of the conventional MPCC and the proposed method is experimentally compared to verify the advantages of the proposed method in weighting factor tuning and digital operation. The results confirm that the proposed method can effectively eliminate the weighting factor in MPCC for five-phase PMSM, providing new schemes to ensure the stable and efficient operation of five-phase PMSM.

The contribution of the proposed method can be summarized as follows:

1) Based on the principle of the cascade MPCC, the proposed method develops two control schemes for five-phase PMSM, namely the maximum torque scheme and the harmonic elimination scheme, to improve the torque response ability and reduce the three harmonic of stator current.

2) For the MPCC of five-phase PMSM, a new way to eliminate weighting factor is presented by the proposed method.

II. MATHEMATIC MODEL OF FIVE-PHASE PMSM

The topology of two-level inverter driving five-phase PMSM is shown in Figure 1. The DC source voltage of the inverter is U_{dc} . By controlling the switches of five-phase bridge arms of the inverter, the AC output side of the inverter will generate five-phase AC currents with phase difference of 72 degree, forming a circular rotating magnetic field in the space to drive the five-phase PMSM.

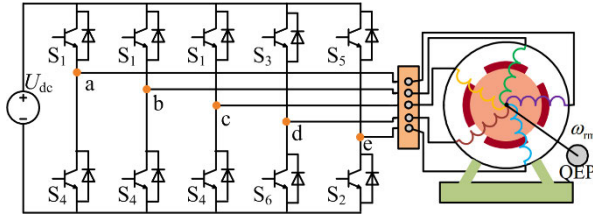


FIGURE 1. Five-phase PMSM driven circuit.

It is assumed that the stator current contains only fundamental and third harmonics currents while ignoring the influence of other higher harmonics. According to the coordinate transformation, the five-phase stator currents i_a, i_b, i_c, i_d, i_e can be equivalent to the currents $i_{d1}, i_{q1}, i_{d3}, i_{q3}$ in the rotating coordinate system, which are expressed by

$$\begin{cases} \frac{di_{d1}}{dt} = -\frac{R_s}{L_d}i_{d1} + \frac{L_q}{L_d}\omega_e i_{q1} + \frac{1}{L_d}u_{d1} \\ \frac{di_{q1}}{dt} = -\frac{R_s}{L_q}i_{q1} - \frac{L_d}{L_q}\omega_e i_{d1} + \frac{1}{L_q}u_{q1} - \frac{\psi_f}{L_q}\omega_e \\ \frac{di_{d3}}{dt} = -\frac{R_s}{L_{ls}}i_{d3} + \frac{1}{L_{ls}}u_{d3} \\ \frac{di_{q3}}{dt} = -\frac{R_s}{L_{ls}}i_{q3} + \frac{1}{L_{ls}}u_{q3} \end{cases} \quad (1)$$

where i_{d1}, i_{q1}, u_{d1} , and u_{q1} are the stator current and voltage components in the dq-axis in fundamental wave space, respectively; i_{d3}, i_{q3}, u_{d3} , and u_{q3} are the stator current and voltage components in the dq-axis in harmonic wave space, respectively; R_s is the stator resistance; L_d and L_q are the stator inductance components in d-axis and q-axis, respectively; L_{ls} is stator leakage inductance; ω_e is the electrical angular velocity of the rotor; ψ_f is the flux linkage of the permanent magnet.

The torque of five-phase PMSM is given as follows

$$T_e = \frac{5}{2}n_p (\psi_{f1}i_{q1} + \psi_{f3}i_{q3}) \quad (2)$$

where ψ_{f1} and ψ_{f3} are the fundamental and harmonic components of permanent magnet flux linkage; n_p is the number of pole pair.

III. CONVENTIONAL MPCC

In this section, the implementation of the conventional MPCC for five-phase PMSM is first introduced. Secondly, the predictive model of stator current is derived from the mathematical model of five-phase PMSM. Thirdly, the principle of selecting the optimal voltage vector by cost function is analyzed.

The structure block diagram of MPCC for five-phase PMSM is presented in Figure 2. The system includes five controlled variables, i.e., the speed n , the fundamental currents i_{d1} and i_{q1} , and the third harmonic currents i_{d3} and i_{q3} . In Figure 2, the speed is controlled by PI regulator while the optimized control for the fundamental and harmonic currents is achieved by the cost function. MPCC will periodically

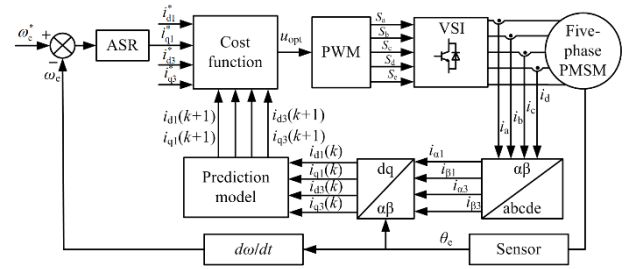


FIGURE 2. Block diagram of model predictive current control for five-phase PMSM.

detect the stator current, predict the system state, select the optimal voltage vector, and therefore realizing on-line rolling optimization. Firstly, the calculated speed error signal is transformed into the reference command i_{q1}^* through the speed regulator. Secondly, the stator current at the current moment is detected, and the fundamental and third harmonic currents at the next moment are calculated according to the prediction model. Thirdly, the predicted values of stator current and their references are sent into the cost function to select the optimal voltage vector that can balance the performance of the fundamental and third harmonic currents. Finally, the optimal voltage vector is converted into the control signal driving the five-phase PMSM.

A. PREDICTION MODEL

According to Euler formula, the continuous model of five-phase PMSM can be expressed by the discrete-time model, which is given as follows

$$\frac{di_{(d1,q1,d3,q3)}(k)}{dt} = \frac{i_{(d1,q1,d3,q3)}(k) - i_{(d1,q1,d3,q3)}(k-1)}{T_s} \quad (3)$$

where T_s, k , and $k-1$ are the control cycle, the current moment, and the previous moment, respectively. The future value of the stator current prediction model is obtained by shifting the time forward one moment, as shown in (4).

$$\begin{cases} i_{d1}(k+1) = \left(1 - \frac{R_s T_s}{L_d}\right) i_{d1}(k) + T_s \omega_e(k) i_{q1}(k) \\ \quad + \frac{T_s}{L_d} u_{d1}(k) \\ i_{q1}(k+1) = \left(1 - \frac{R_s T_s}{L_q}\right) i_{q1}(k) - T_s \omega_e(k) i_{d1}(k) \\ \quad + \frac{T_s}{L_q} u_{q1}(k) - \frac{T_s \psi_f}{L_q} \omega_e(k) \\ i_{d3}(k+1) = \left(1 - \frac{R_s T_s}{L_{ls}}\right) i_{d3}(k) + \frac{T_s}{L_{ls}} u_{d3}(k) \\ i_{q3}(k+1) = \left(1 - \frac{R_s T_s}{L_{ls}}\right) i_{q3}(k) + \frac{T_s}{L_{ls}} u_{q3}(k) \end{cases} \quad (4)$$

where $i_{d1}(k+1), i_{q1}(k+1), i_{d3}(k+1)$, and $i_{q3}(k+1)$ are the predicted stator current components in the dq-axis in fundamental and harmonic wave spaces, respectively. $u_{d1}(k), u_{q1}(k), u_{d3}(k)$, and $u_{q3}(k)$ are the stator voltage components

TABLE 1. Basic voltage vector classification.

Category (voltage vector)	Voltage vector
zero	U_0, U_{31}
small	$U_{21}, U_{22}, U_{23}, U_{24}, U_{25}, U_{26}, U_{27}, U_{28}, U_{29}$ $, U_{30}$
medium	$U_{11}, U_{12}, U_{13}, U_{14}, U_{15}, U_{16}, U_{17}, U_{18}, U_{19}$ $, U_{20}$
large	$U_1, U_2, U_3, U_4, U_5, U_6, U_7, U_8, U_9, U_{10}$

in the dq-axis in fundamental and harmonic wave spaces, respectively

There are totally 32 voltage vectors generated through the five-phase bridge arms. The 32 basic voltage vectors provide a rich control set for MPCC. The control set can be composed of large vector and zero vector, or large vector, medium vector and zero vector, or all vectors. The more the voltage vectors in the control set, the better the control performance. However, selecting the optimal voltage vector by enumeration method causes a great computational burden to the microprocessor. Therefore, MPCC for five-phase PMSM usually needs to balance the amount of computation and control performance.

B. COST FUNCTION

After the prediction of each controlled variables, the predicted and reference values of all controlled variables are substituted into the cost function to quantify the system control error at the next moment. To form a cost function g , $i_{d1}(k+1)$, $i_{q1}(k+1)$, $i_{d3}(k+1)$, and $i_{q3}(k+1)$ in (4) are compared with their references and match a weighting factor λ . The cost function is given as follows

$$g = |i_{d1}^* - i_{d1}(k+1)| + |i_{q1}^* - i_{q1}(k+1)| + \lambda \left[|i_{d3}^* - i_{d3}(k+1)| + |i_{q3}^* - i_{q3}(k+1)| \right] \quad (5)$$

where λ is weighting factor of the third harmonic current that can be tuned for balancing the performance of i_d and i_q ; i_{d1}^* , i_{q1}^* , i_{d3}^* , and i_{q3}^* are the references of the fundamental and third harmonic currents. By using (5), the cost function value of each voltage vector can be calculated. The smaller the cost function value, the smaller the sum of control errors, and the better the control performance of the system. Therefore, the voltage vector with the smallest cost function is the optimal one for the system.

IV. CASCADE MPCC FOR FIVE-PHASE PMSM

MPCC for five-phase PMSM are with simple principle and fast dynamic response, but faces the problems of difficult to adjust the weighting factor and large amount of calculation. On the one hand, the performance of fundamental current and third harmonic current needs to be balanced by setting a proper weighting factor in the cost function. However, due to lacking of theoretical basis, the weighting factor is mainly obtained by the tedious trial and error method based on the

analysis of a large number of experimental data. Furthermore, the unreasonable weighting factor may be used when the motor parameter or the system operation changes, leading to a wrong selection of the optimal voltage vector. On the other hand, the system state prediction and the optimal voltage vector selection from 32 voltage vectors bring a great computational burden to the microprocessor.

To solve the problems above, a cascade MPCC for five-phase PMSM is proposed. The cost function including fundamental current and third harmonic current is divided into two independent cost functions. The two cost functions are combined according to the priority of controlled variables, selecting the optimal voltage vector step by step. In addition, to reduce the computation of the proposed algorithm, the sector judgment method is used to eliminate unreasonable voltage vectors. In this section, the proposed method will be introduced in detail from four aspects, i.e., the control principle, the cost function design, the voltage vector selection, and delay compensation.

A. PRINCIPLE OF PROPOSED METHOD

Due to the currents i_{d1} and i_{q1} in the fundamental space and the currents i_{d3} and i_{q3} in the harmonic space included in the same cost function, the performance optimization needs to take into account multiple controlled variables at the same time. Therefore, the parallel approach is adopted for the selection of voltage vector. Based on the idea of sequential MPC, the parallel approach is transformed into cascade one, and a cascade MPCC is proposed. In the proposed method, independent cost function is designed for each controlled variable. The cost functions are prioritized according to the importance of the controlled variables and then combined in series. Therefore, the primary and secondary relation of the controlled variables in the system can be clearly distinguished by the new cost function, which is the basis for selecting the voltage vector. The controlled variable with the top importance can first select some voltage vectors with good performance by its cost function. Then, the controlled variable with the bottom priority selects a voltage vectors with smaller cost function value from the voltage vectors in the first step. After step-by-step selection, the optimal voltage vector considering the performance of each controlled variable can be obtained.

The structural block diagram of the proposed method is shown in Figure 3. The speed control is consistent with that in the traditional MPCC using a PI regulator while the stator fundamental and third harmonic currents are controlled using a cascade cost function. Firstly, the reference and predicted values of fundamental and third harmonic current components in dq-axis are calculated for the one-step delay compensation and the reference voltage vector location. Secondly, the cost function of each controlled variable is built. The priority of the cost functions of fundamental current and third harmonic current is established according to the control performance requirements of the system. Finally, the basic voltage vector is evaluated by the high priority cost function to select two optimal voltage vectors u_{opt1} and u_{opt2} , and then the two

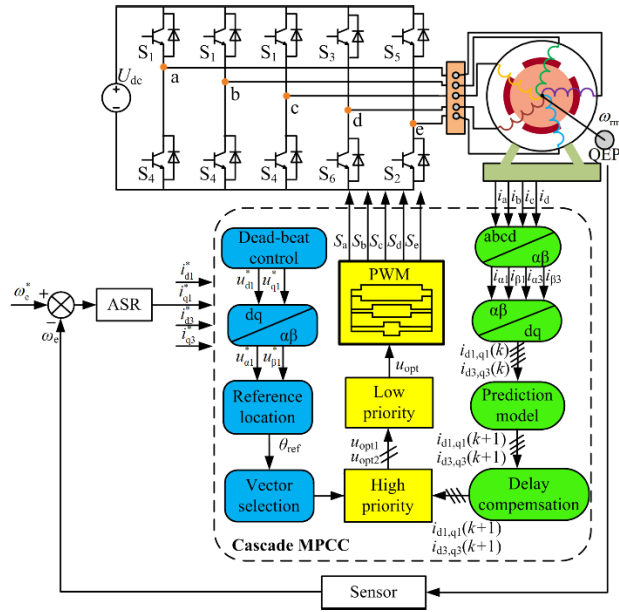


FIGURE 3. Structure block diagram of cascade model predictive current control of five-phase PMSM.

voltage vectors are evaluated by the low priority cost function to select the optimal voltage vector u_{opt} .

The advantage of the proposed method is that the selection of optimal voltage vector is completed by two steps according to the priority of cost function, without taking into account the performance of the fundamental and third harmonic currents at the same time. Since optimal control is only for one controlled variable in one step, the selection of the optimal voltage vector does not depend on the weighting factor.

B. CASCADE COST FUNCTION DESIGN

The cost function of the proposed method obtained from (5) can achieve the independently control of the stator fundamental current and the third harmonic current. The cost function of the fundamental current includes i_{d1} , i_{q1} , i_{d1}^* , and i_{q1}^* while the cost function of the third harmonic current consists of i_{d3} , i_{q3} , i_{d3}^* , and i_{q3}^* . Their expressions are as follows

$$g_{d1} = |i_{d1}^* - i_{d1}(k+1)| + |i_{q1}^* - i_{q1}(k+1)| \quad (6)$$

$$g_{d3} = |i_{d3}^* - i_{d3}(k+1)| + |i_{q3}^* - i_{q3}(k+1)| \quad (7)$$

Using equations (6) and (7), the optimal voltage vector for effectively controlling the fundamental and third harmonic currents can be selected. In this paper, a cascade combination of the two cost functions can balance the system performance from the perspectives of maximum torque and minimum harmonic current.

1) MAXIMUM TORQUE SCHEME

The goal of the maximum torque scheme is to increase the output torque of PMSM. Therefore, the cost function of the fundamental current has the highest priority, followed by

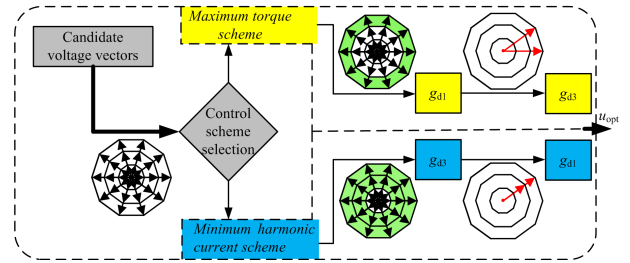


FIGURE 4. Cost function design in cascade model predictive current control.

that of the third harmonic current, as shown in Figure 4. As the high DC voltage utilization causes large torque, the optimal voltage vector should be selected from large vector and zero vector. For this reason, 10 large vectors and one zero vector among the 32 basic voltage vectors are used as candidate voltage vectors for the maximum torque scheme. Firstly, using the cost function of the fundamental current, two large vectors and a zero vector that minimize g_{d1} are selected from as the candidate vectors of the cost function of third harmonic current. Secondly, after calculating the values of the cost function of the third harmonic current under the three voltage vectors, the voltage vector that minimizes g_{d3} is selected as the optimal voltage vector of the maximum torque scheme.

2) MINIMUM HARMONIC CURRENT SCHEME

The objective of the minimum harmonic current scheme is to reduce the torque ripple. Contrary to the maximum torque scheme, the minimum harmonic current scheme makes the cost function of third harmonic current have the highest priority, followed by the cost function of fundamental current, as shown in Figure 4. Since the third harmonic current results in torque ripple, the optimal voltage vector should be selected from large vector, medium vector and zero vector. For this reason, 10 large vectors, 10 medium vectors, and one zero vector among the 32 basic voltage vectors are used as candidate voltage vectors of the minimum harmonic current scheme. Firstly, a voltage vector from the large vector, a voltage vector from the medium vector, and one zero vector minimizing the cost function of third harmonic current are selected as the input of the cost function of fundamental current. Secondly, after calculating the values of the cost function of the fundamental current under the three voltage vectors, the voltage vector that minimizes g_{d1} is selected as the optimal voltage vector of the minimum harmonic current method.

C. VOLTAGE VECTOR SELECTION

The proposed maximum torque scheme and minimum harmonic current scheme can reduce the candidate voltage vectors from 32 to 11 and 21, respectively, reducing the amount of calculation of MPCC. However, the number of candidate voltage vectors is still large for the implementation of control method in microprocessor. Therefore, the sector location

method is used to quickly select some useful voltage vectors from all the voltage vectors.

To make the stator current accurately track the reference command, the predicted value of fundamental current is equal to the reference value. Inversely derived by (4), the desired fundamental output voltage can be expressed by

$$\begin{cases} u_{d1}^* = \frac{L_d}{T_s} \left[i_{d1}^* - \left(1 - \frac{R_s T_s}{L_d} \right) i_{d1}(k) - T_s \omega_e(k) i_{q1}(k) \right] \\ u_{q1}^* = \frac{L_d}{T_s} \left[i_{q1}^* - \left(1 - \frac{R_s T_s}{L_d} \right) i_{q1}(k) + T_s \omega_e(k) i_{d1}(k) \right] \\ \quad + \frac{T_s \psi_f}{L_q} \omega_e(k) \end{cases} \quad (8)$$

where, u_{d1}^* and u_{q1}^* are the components of the output voltage reference in the fundamental space. The rotating coordinate system can be transformed into the stationary one by using ipark transformation, and thus the output voltage are obtained as

$$\begin{bmatrix} u_{\alpha}^* \\ u_{\beta}^* \end{bmatrix} = \begin{bmatrix} \cos \theta_e & -\sin \theta_e \\ \sin \theta_e & \cos \theta_e \end{bmatrix} \begin{bmatrix} u_{d1}^* \\ u_{q1}^* \end{bmatrix} \quad (9)$$

where θ_e is electrical angle According to (9), the phase angle of the reference voltage vector is located using the arctangent function, which is

$$\theta_{ref} = \arctan \frac{u_{\beta}^*}{u_{\alpha}^*} \quad (10)$$

As for (10), the adjacent voltage vectors of the sector located using the reference voltage vector are applied to improve the control accuracy of stator current. Therefore, 4 large vectors and one zero vector close to the reference voltage vector are used as candidate voltage vectors for the maximum torque scheme. 2 large vectors and 2 medium vectors close to the reference voltage vector and one zero vector are taken as the candidate voltage vectors for the minimum harmonic current scheme.

It can be seen that the number of the candidate voltage vectors of the proposed method and the conventional one are 5 and 32, respectively. 27 candidate voltage vectors are reduced in proposed method compared with that of the conventional one, decreasing the amount of calculation by 84%.

D. IMPLEMENTATION OF PROPOSED METHOD

As shown in Figure 5, the implementation of cascade MPCC for five-phase PMSM can be divided into 5 steps.

Step 1: measure the stator current and the speed of five-phase PMSM, calculate the reference command, and predict the system state.

Step 2: use (14) to compensate one-step delay for stator fundamental current and third harmonic current.

Step 3: locate the sector of the reference voltage vector and select the adjacent voltage vector of the sector as the candidate voltage vector.

Step 4: select the control scheme according to the requirements of control performance, design the priority of cost function, and construct cascade cost function.

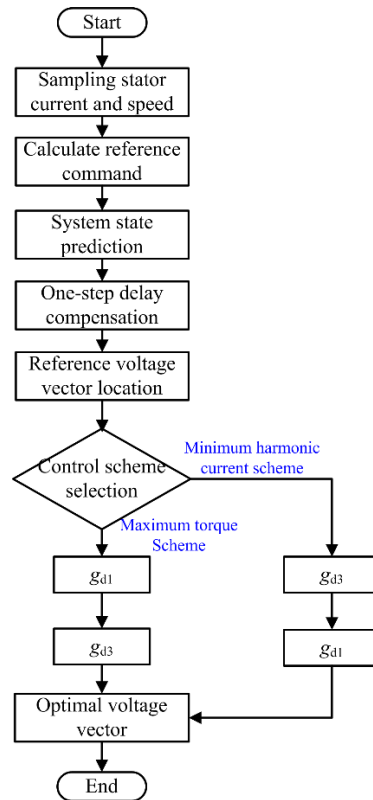


FIGURE 5. Flow chart of cascade model predictive current control.

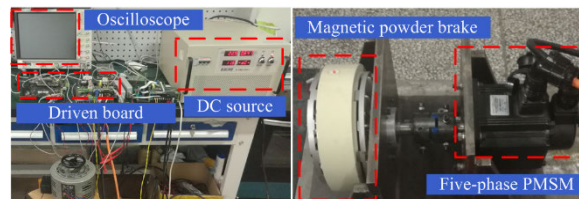


FIGURE 6. Five-phase PMSM experimental setup.

Step 5: convert the optimal voltage vector into PWM control signal driving five phase PMSM.

V. EXPERIMENTAL RESULTS

To verify the correctness and the advantages of the proposed method, the experiments of the performance comparison among the proposed method, the conventional MPCC, and the MPCC with virtual voltage vector in [23] are carried out on the five-phase PMSM setup. As shown in Figure 6, a DSP TMS TMS320F28335 is used as the micro-processor executing the control algorithm. A five-phase PMSM is connected to a magnetic powder brake generating the load torque. The parameters of five-phase PMSM are in TABLE 2.

The weighting factor λ for the conventional MPCC is tuned using the trial-and-error approach. Based on large numbers of experimental tests, the value of λ is set to 1.9. The experimental results are shown in Figure 7~Figure 11.

TABLE 2. Experimental parameters.

Quantity	Value	Unit
rate speed	1200	r/min
rate current	10	A
stator inductance	6.2	mH
stator resistance	0.42	Ω
flux linkage	0.157	Wb
pole pairs	4	-
control cycle	40	μ s

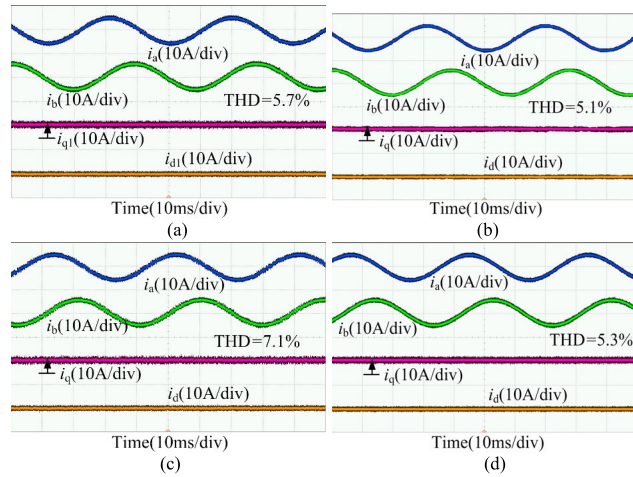


FIGURE 7. Steady-state experimental results. (a) Maximum torque scheme, (b) minimum harmonic current scheme, (c) conventional MPCC, and (d) MPCC with virtual voltage vector.

A. STEADY-STATE EXPERIMENTAL RESULTS

The steady-state experiment at the speed of 380r/min are carried out to compare the current harmonics of the maximum torque scheme, minimum harmonic current scheme, conventional MPCC, and MPCC with virtual voltage vector, as shown in Figure 7. It can be clearly seen that smooth currents are obtained in the minimum harmonic current scheme and MPCC with virtual voltage vector, while the harmonic current can be observed in the maximum torque scheme and conventional MPCC. From the total harmonic distortion analysis (THD), the current THD of the minimum harmonic current scheme is 5.1%, smaller than that of the maximum torque scheme 5.7%, that of the conventional MPCC 7.1%, and that of MPCC with virtual voltage vector 5.3%.

B. EXPERIMENT OF STEP CHANGE IN SPEED

The experiment of step change in speed is made to compare the dynamic response of the maximum torque scheme, minimum harmonic current scheme, conventional MPCC, and MPCC with virtual voltage vector, as shown in Figure 8 and Figure 9. In Figure 8, the speed is changed from 200 r/min to 1200r/min spending about 120 ms in the three methods. Therefore, the speed response of the four methods is the same. In Figure 9, q-axis current in the start of speed change is presented. The q-axis currents of the maximum torque

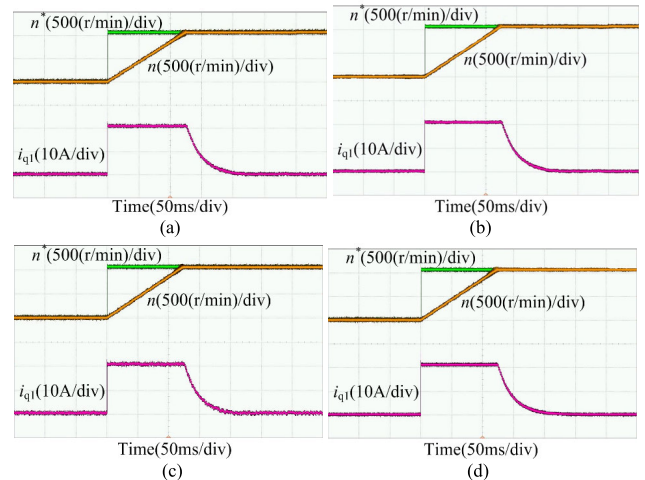


FIGURE 8. Speed dynamic experimental results. (a) Maximum torque scheme, (b) minimum harmonic current scheme, (c) conventional MPCC, and (d) MPCC with virtual voltage vector.

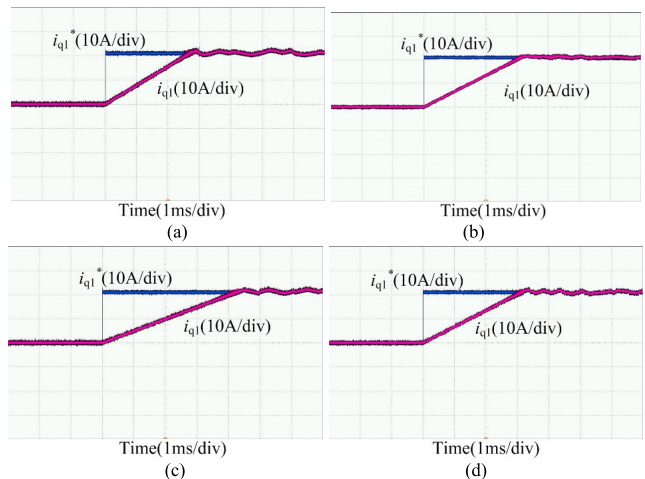


FIGURE 9. Zoom view of q-axis current in the speed dynamic experimental results. (a) Maximum torque scheme, (b) minimum harmonic current scheme, (c) conventional MPCC, and (d) MPCC with virtual voltage vector.

scheme, the minimum harmonic current scheme, and MPCC with virtual voltage vector track their references in 2.9 ms, 3.2 ms, and 3.3 ms, obtaining fast current response. However, the conventional MPCC has a relative slow current response completing within 4.5 ms.

C. EXPERIMENT OF LOAD DISTURBANCE

The experiment results of load disturbance using the maximum torque scheme, minimum harmonic current scheme, conventional MPCC, and MPCC with virtual voltage vector are shown in Figure 10. When the machine operates at 1100r/min, the magnetic powder brake generates a load torque. It can be observed that the maximum torque scheme has a fast current response and a small speed drop, exhibiting a good dynamic performance against the load disturbance over the minimum harmonic current scheme, the conventional MPCC, and the MPCC with virtual voltage vector.

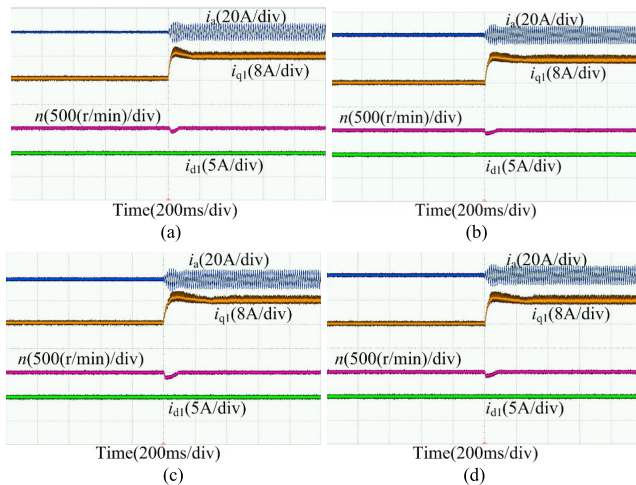


FIGURE 10. Load disturbance experimental results. (a) Maximum torque scheme, (b) minimum harmonic current scheme, (c) conventional MPCC, and (d) MPCC with virtual voltage vector.

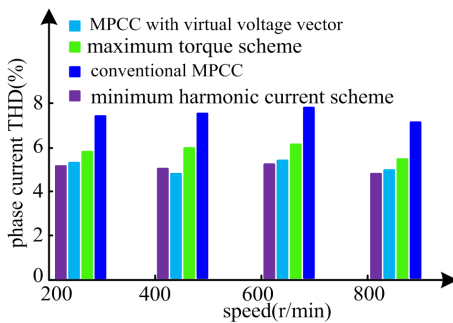


FIGURE 11. Stator current THD at different speed.

TABLE 3. Experimental result summarizing.

Method	Current respond time	Speed drop
Maximum torque scheme	2.9ms	60r/min
Minimum harmonic current scheme	3.2ms	80r/min
Conventional MPCC	3.3ms	90r/min
MPCC with virtual voltage vector	4.5ms	120r/min

D. EXPERIMENT PERFORMANCE EVALUATION

The stator current THD of the four MPC methods are compared at different speed to verify the advantage of proposed method, as shown in Figure 11. At 200r/min, 400r/min, 600r/min, and 800r/min, the stator current THD of the proposed maximum torque scheme, the proposed minimum harmonic current scheme, the conventional MPCC, and the MPCC with virtual voltage vector changes little. The proposed minimum harmonic current scheme has the same current THD with the MPCC with virtual voltage vector, smaller than the other two methods. Therefore, the proposed minimum harmonic current scheme can effectively lower current THD.

The dynamic performance in part B and the performance against load disturbance in part C are summarized in TABLE 3. The current response time of the proposed

maximum torque scheme, the proposed minimum harmonic current scheme, the conventional MPCC, and the MPCC with virtual voltage vector are 2.9ms, 3.2ms, 3.3 ms, and 4.5ms, respectively, while their speed drop in loading test are 60r/min, 80r/min, 90r/min, and 120r/min. It can be clearly seen that the proposed maximum torque scheme has the best dynamic performance and the ability against load disturbance among the four methods.

VI. CONCLUSION

This paper proposes a cascade MPCC for five-phase PMSM to solve the problem of tedious tuning work of weighing factor. Through setting the control priority of fundamental current and harmonics current to form the cascade structure of the cost function, the optimal voltage vector used to balance the performance of the fundamental current and the harmonics current can be selected without using a weighting factor. The construction scheme of cost function can be changed with the system performance requirement, developing to a maximum torque scheme for output electromagnetic torque improvement and a harmonic elimination scheme for eliminating third harmonic in stator current. The Experimental results indicate that the proposed method is better than the conventional MPCC in dynamic performance and current harmonic elimination without weighting factor.

REFERENCES

- [1] S. M. Ahmed, H. Abu-Rub, and Z. Salam, "Common-mode voltage elimination in a three-to-five-phase dual matrix converter feeding a five-phase open-end drive using space-vector modulation technique," *IEEE Trans. Ind. Electron.*, vol. 62, no. 10, pp. 6051–6063, Oct. 2015.
- [2] T. Tao, W. Zhao, Y. He, Y. Cheng, S. Saeed, and J. Zhu, "Enhanced fault-tolerant model predictive current control for a five-phase PM motor with continued modulation," *IEEE Trans. Power Electron.*, vol. 36, no. 3, pp. 1–5, Mar. 2021.
- [3] A. Bhowate, M. V. Aware, and S. Sharma, "Predictive torque control algorithm for a five-phase induction motor drive for reduced torque ripple with switching frequency control," *IEEE Trans. Power Electron.*, vol. 35, no. 7, pp. 7282–7294, Jul. 2020.
- [4] Y. N. Tatte and M. V. Aware, "Torque ripple and harmonic current reduction in a three-level inverter-fed direct-torque-controlled five-phase induction motor," *IEEE Trans. Ind. Electron.*, vol. 64, no. 7, pp. 5265–5275, Jul. 2017.
- [5] M. Priestley, J. E. Fletcher, and C. Tan, "Space-vector PWM technique for five-phase open-end winding PMSM drive operating in the overmodulation region," *IEEE Trans. Ind. Electron.*, vol. 65, no. 9, pp. 6816–6827, Sep. 2018.
- [6] J. Rodríguez, M. P. Kazmierkowski, J. R. Espinoza, P. Zanchetta, H. Abu-Rub, H. A. Young, and C. A. Rojas, "State of the art of finite control set model predictive control in power electronics," *IEEE Trans. Ind. Informat.*, vol. 9, no. 2, pp. 1003–1016, May 2013.
- [7] P. Karamanakos, T. Geyer, and R. P. Aguilera, "Long-horizon direct model predictive control: Modified sphere decoding for transient operation," *IEEE Trans. Ind. Appl.*, vol. 54, no. 6, pp. 6060–6070, Nov./Dec. 2018.
- [8] S. Vazquez, J. Rodríguez, M. Rivera, L. G. Franquelo, and M. Norambuena, "Model predictive control for power converters and drives: Advances and trends," *IEEE Trans. Ind. Electron.*, vol. 64, no. 2, pp. 935–947, Feb. 2017.
- [9] B. Yu, W. Song, J. Li, B. Li, and M. S. R. Saeed, "Improved finite control set model predictive current control for five-phase VSIs," *IEEE Trans. Power Electron.*, vol. 36, no. 6, pp. 7038–7048, Jun. 2021.
- [10] M. Mamdouh and M. A. Abido, "Efficient predictive torque control for induction motor drive," *IEEE Trans. Ind. Electron.*, vol. 66, no. 9, pp. 6757–6767, Sep. 2019.

- [11] Y. Xu, Y. He, and S. Li, "Logical operation-based model predictive control for quasi-z-source inverter without weighting factor," *IEEE J. Emerg. Sel. Topics Power Electron.*, vol. 9, no. 1, pp. 1039–1051, Feb. 2021.
- [12] J. J. Aciego, I. G. Prieto, and M. J. Duran, "Model predictive control of six-phase induction motor drives using two virtual voltage vectors," *IEEE J. Emerg. Sel. Topics Power Electron.*, vol. 7, no. 1, pp. 321–330, Mar. 2019.
- [13] Y. He and Y. Xu, "Dynamic model predictive current control based on deviation for permanent magnet synchronous motor," in *Proc. IEEE 28th Int. Symp. Ind. Electron. (ISIE)*, Vancouver, BC, Canada, Jun. 2019, pp. 313–317.
- [14] M. Cheng, F. Yu, K. T. Chau, and W. Hua, "Dynamic performance evaluation of a nine-phase flux-switching permanent-magnet motor drive with model predictive control," *IEEE Trans. Ind. Electron.*, vol. 63, no. 7, pp. 4539–4549, Jul. 2016.
- [15] J. Rodriguez *et al.*, "Latest advances of model predictive control in electrical drives—Part I: Basic concepts and advanced strategies," *IEEE Trans. Power Electron.*, vol. 37, no. 4, pp. 3927–3942, Apr. 2022.
- [16] R. Vargas, P. Cortes, U. Ammann, J. Rodriguez, and J. Pontt, "Predictive control of a three-phase neutral-point-clamped inverter," *IEEE Trans. Ind. Electron.*, vol. 54, no. 5, pp. 2697–2705, Oct. 2007.
- [17] P. Cortes, S. Kouro, B. La Rocca, R. Vargas, J. Rodriguez, J. I. Leon, S. Vazquez, and L. G. Franquelo, "Guidelines for weighting factors design in model predictive control of power converters and drives," in *Proc. IEEE Int. Conf. Ind. Technol.*, Churchill, VIC, Australia, Feb. 2009, pp. 1–7.
- [18] M. Novak, H. Xie, T. Dragicevic, F. Wang, J. Rodriguez, and F. Blaabjerg, "Optimal cost function parameter design in predictive torque control (PTC) using artificial neural networks (ANN)," *IEEE Trans. Ind. Electron.*, vol. 68, no. 8, pp. 7309–7319, Aug. 2021.
- [19] O. Machado, P. Martín, F. J. Rodríguez, and E. J. Bueno, "A neural network-based dynamic cost function for the implementation of a predictive current controller," *IEEE Trans. Ind. Informat.*, vol. 13, no. 6, pp. 2946–2955, Dec. 2017.
- [20] R. S. Dastgerdi, M. A. Abbasian, H. Saghafi, and M. H. Vafaie, "Performance improvement of permanent-magnet synchronous motor using a new deadbeat-direct current controller," *IEEE Trans. Power Electron.*, vol. 34, no. 4, pp. 3530–3543, Apr. 2019.
- [21] C. A. Rojas, J. Rodriguez, F. Villarroel, J. R. Espinoza, C. A. Silva, and M. Trincado, "Predictive torque and flux control without weighting factors," *IEEE Trans. Ind. Electron.*, vol. 60, no. 2, pp. 681–690, Feb. 2013.
- [22] M. Norambuena, J. Rodriguez, Z. Zhang, F. Wang, C. Garcia, and R. Kennel, "A very simple strategy for high-quality performance of AC machines using model predictive control," *IEEE Trans. Power Electron.*, vol. 34, no. 1, pp. 794–800, Jan. 2019.
- [23] X. Wu, W. Song, and C. Xue, "Low-complexity model predictive torque control method without weighting factor for five-phase PMSM based on hysteresis comparators," *IEEE J. Emerg. Sel. Topics Power Electron.*, vol. 6, no. 4, pp. 1650–1661, Dec. 2018.
- [24] C. Gong, Y. Hu, J. Gao, Y. Wang, and L. Yan, "An improved delay-suppressed sliding-mode observer for sensorless vector-controlled PMSM," *IEEE Trans. Ind. Electron.*, vol. 67, no. 7, pp. 5913–5923, Jul. 2020.



SHU XIONG was born in Jiangsu, China. He received the M.S. degree in power electronics and drives from the China University of Mining and Technology, in 2006. He is currently pursuing the Ph.D. degree in electrical engineering with the Nanjing University of Aeronautics and Astronautics, Nanjing, China. He joined as a Lecturer at HNU, in 2006. He has been an Associate Professor with Huaiyin Normal University, since 2014. His research interests include multi-level power converter for power conversion and motor control and high-efficiency converter for renewable power conversion systems.



JIANGCHENG LI was born in Jiangsu, China. He received the M.S. degree in power electronics and drives from the China University of Mining and Technology, in 2005. He joined at State Grid Suqian Power Supply Company, in 2005, where he was a Senior Engineer, from 2011 to 2020. He is currently the Vice General Manager of State Grid Huaian Power Supply Company, Jiangsu. His current research interests include resonant converters and wireless power transfer systems, motor control, and high-efficiency converter for renewable power conversion systems.

• • •